



Comparative Performance of Microbial Desalination Cells Using Air Diffusion and Liquid Cathode Reactions: Study of the Salt Removal and Desalination Efficiency

Marina Ramírez-Moreno¹, Pau Rodenas¹, Martí Aliaguilla², Pau Bosch-Jimenez², Eduard Borràs², Patricia Zamora^{3*}, Víctor Monsalvo³, Frank Rogalla³, Juan M. Ortiz^{1*} and Abraham Esteve-Núñez^{1,4}

OPEN ACCESS

Edited by:

Uwe Schröder,
Technische Universität
Braunschweig, Germany

Reviewed by:

Carlo Santoro,
University of the West of England,
United Kingdom
Mohanakrishna Gunda,
Qatar University, Qatar

*Correspondence:

Patricia Zamora
patricia.zamora@fcc.es
Juan M. Ortiz
juanma.ortiz@imdea.org

Specialty section:

This article was submitted to
Bioenergy and Biofuels,
a section of the journal
Frontiers in Energy Research

Received: 25 July 2019

Accepted: 11 November 2019

Published: 05 December 2019

Citation:

Ramírez-Moreno M, Rodenas P, Aliaguilla M, Bosch-Jimenez P, Borràs E, Zamora P, Monsalvo V, Rogalla F, Ortiz JM and Esteve-Núñez A (2019) Comparative Performance of Microbial Desalination Cells Using Air Diffusion and Liquid Cathode Reactions: Study of the Salt Removal and Desalination Efficiency. *Front. Energy Res.* 7:135. doi: 10.3389/fenrg.2019.00135

¹ IMDEA Water Institute, Parque Científico Tecnológico de la Universidad de Alcalá, Alcalá de Henares, Spain, ² LEITAT Technological Center, Barcelona, Spain, ³ FCC Aqualia S.A., Madrid, Spain, ⁴ Department of Analytical Chemistry, Physical Chemistry and Chemical Engineering Department, Universidad de Alcalá, Alcalá de Henares, Spain

Microbial Desalination Cell (MDC) represents an innovative technology which accomplishes simultaneous desalination and wastewater treatment without external energy input. MDC technology could be employed to provide freshwater with low-energy input, for example, in remote areas where organic wastes (i.e., urban or industrial) are available. In addition, MDC technology has been proposed as pre-treatment in conventional reverse osmosis plants, with the aim of saving energy and avoiding greenhouse gases related to conventional desalination processes. The use of oxygen reduction (i.e. $O_2 + 2H_2O + 4e^- \rightarrow 4 OH^-$, $E^0 = 0.815V$, $pH = 7$) was usually implemented as cathodic reaction in most of the MDCs reported in literature, whereas other strategies based on liquid catholytes have been also proposed, for example, ferro-ferricyanide redox couple (i.e. $Fe(CN)_6^{3-} + 1e^- \rightarrow Fe(CN)_6^{4-}$, $E^0 = 0.37V$). As the MDC designs in the literature and operation modes (i.e., batch, continuous, semi-continuous, etc.) are quite different, the available MDC studies are not directly comparable. For this reason, the main objective of this work was to have a proper comparison of two similar MDCs operating with two different catholyte strategies, and compare performance and desalination efficiencies. In this sense, this study compares the desalination performance of two laboratory-scale MDCs located in two different locations for brackish water and sea water using two different strategies. The first strategy consisted of an air cathode for efficient oxygen reduction, while the second strategy was based on a liquid catholyte with Fe^{3+}/Fe^{2+} solution (i.e., ferro-ferricyanide complex). Both strategies achieved desalination efficiency above 90% for brackish water. Nominal desalination rates (NDR) were in the range of 0.17–0.14 $L \cdot m^{-2} \cdot h^{-1}$ for brackish and seawater with air diffusion cathode MDC, respectively, and 1.5–0.7 $L \cdot m^{-2} \cdot h^{-1}$ when using ferro-ferricyanide redox MDC. Organic matter present in wastewater was effectively removed at 0.9 and 1.1 $kg \text{ COD} \cdot m^{-3} \cdot day^{-1}$ using the air diffusion cathode MDC for brackish and

sea water, respectively, and 7.1 and 19.7 kg COD·m⁻³·day⁻¹ with a ferro-ferricyanide redox MDC. Both approaches used a laboratory MDC prototype without any energy supply (excluding pumping energy). Pros and cons of both strategies are discussed for subsequent upscaling of MDC technology.

Keywords: microbial desalination cell, wastewater treatment, air cathode, sea water, brackish water

INTRODUCTION

More than 700 million people worldwide do not have access to enough clean water and the number is expected to rise up to 1.8 billion people in the next decade (Talbot, 2015). The water sources in regions like the Mediterranean coast, Mexican Gulf or California coast start to be depleted by an increasing demand of drinking water, agriculture, or industry use, while the Middle East region, one of the most water-scarce regions of the world, copes with similar water scarcity problems (Water Scarcity, 2019). Consequently, current desalination technologies have a huge impact on society due to the increasing demand of water worldwide (Badiuzzaman et al., 2017; Chowdhury et al., 2018). However, the high energy cost continues to be a major concern, with energy consumption accounting for 75% of the desalination operating costs when excluding capital costs, or 40% including capital costs (Elmekawy et al., 2014). This energy cost for desalination is about 10 times higher than for conventional water sources, leading to high water prices.

In this context, the most extended desalination technology is reverse osmosis (RO) with an associated energy consumption of 3.5 kWh·m⁻³ (50% recovery) (MacHarg et al., 2008). Temperature-driven technologies such as multi stage flash (MSF) and multi effect distillation (MED) consume even larger amounts of energy (5.5–40 kWh·m⁻³), thus limiting their use only in countries with low fuel cost (Sharon and Reddy, 2015). Electrodialysis (ED) desalination is mainly suitable for brackish water applications since energy costs depends on the salinity of the water source (Ortiz et al., 2005). Other emerging membrane technologies like forward osmosis (FO), membrane distillation (MD), and capacitive deionization (CDI) have been shown to be only suitable for specific treatment applications (Yuan et al., 2012; Shaffer et al., 2014; Wang and Chung, 2015).

Microbial Desalination Cell (MDC) is a novel technology able to produce sustainable drinking water by using the energy provided from the metabolism of electroactive bacteria when organic matter is degraded, allowing simultaneous desalination of water, treatment of waste water and production of electricity. MDC consists of an electrochemical device with three compartments (Cao et al., 2009). The anodic compartment comprises an electrode covered by a biofilm that oxidizes the organic matter contained in the wastewater, transferring electrons from the substrate (i.e., organic matter) to the electrode. Then, the electrons use an external circuit to reach the cathodic compartment, where the reduction reaction takes place. The electric potential forces the migration of ions. Therefore, desalination takes place when positive ions move through the cation exchange membrane (CEM) from the saline

compartment to the cathode and negative ions move through the anion exchange membrane (AEM) from saline to the anodic compartment.

The first concept of MDC was proposed by Cao et al. in a cell of 9 cm² (cross section) with a saline volume chamber of 11 mL, achieving 90% of salt removal batchwise, at initial salt concentrations ranging from 5 to 35 NaCl g·L⁻¹ (Cao et al., 2009). Different MDC configurations have been reported in the literature, including cubic and tubular reactors (Mehanna et al., 2010; Jacobson et al., 2011a,b; Ping and He, 2013), stacked cells (Chen et al., 2011; Kim and Logan, 2011), using batch recirculation (Chen et al., 2012; Qu et al., 2012), biocathodes (Wen et al., 2012), increasing water production by applying external voltage (Ge et al., 2014), or integrating innovative membranes (forward osmosis) (Zhang and He, 2012; Yuan et al., 2015), ion exchange resins in the compartments (Zhang et al., 2012), or microfiltration processes (Zuo et al., 2017, 2018). Up to date, the biggest MDC ever built (100 L) was reported to achieve partial desalination of sea water with a nominal desalination rate of 0.077 L·m⁻²·h⁻¹ (Zhang and He, 2015).

Cathode reaction is considered one of the main bottlenecks in microbial electrochemical technologies (METs) (Freguia et al., 2008). Most of the MDC studies have been carried out by implementing oxygen reduction in the cathodic compartment by taking advantage of the gained experience in the field of microbial electrochemical systems using oxygen as electron acceptor (i.e. $O_2 + 2H_2O + 4e^- \rightarrow 4 OH^-$, $E^0 = 0.815 V$, pH = 7). Current challenges are to develop air-cathodes with high oxygen reduction reaction (ORR) performance, long term stability and low cost (Freguia et al., 2007; Lu and Li, 2012). Zhao et al. studied three main factors that affect air cathodes performance: the solution pH, the catholyte concentration and the catalyst load (Zhao et al., 2006). Precious metals (Pt, Pd, Au, or Ag) are used as catalysts in electrochemical devices to reduce oxygen in different pH conditions (Ge et al., 2015). Liu et al. showed operative oxygen reduction potential on MFCs between 0.17 to 0.26 V using MnOx as alternative catalyst instead of precious metals (i.e., Pt, Pd) (Zhao et al., 2006; Liu et al., 2010). Also other metal oxides or metal-organic catalysts from the transition metal group (FeOOH, CoOOH, MnOx, WO₃, Co-PPY) have been developed to reduce the capital costs (Bashyam and Zelenay, 2006; Lu and Li, 2012; Wang et al., 2015; Zhang et al., 2016). Among these transition metals, nickel has been shown good performance when surface properties are modified to facilitate ORR (Vij et al., 2017). Additionally, iron is also another promising transition metal for ORR on microbial electrochemical devices (Lefèvre et al., 2009). For example, Harnish et al. demonstrated the versatility of iron-phthalocyanine as catalyst for oxygen reduction on MFCs at

TABLE 1 | Main features for MDC experimental setups.

Location	LEITAT Lab	IMDEA Water Lab
Cross section (cm ²)	100	100
Dimensions active area (cm)	10 × 10	10 × 10
Number of unit cells	1	1
ANODE		
Electric collector	Stainless steel	Isostatic graphite plate (Grade 2114-45)
Electrode	SGL Unidirectional Carbon Fiber Felt	RVG 2000 MERSEN Carbon Felt
Electrode thickness (mm)	5.0	4.6
Compartment thickness (mm)	8.7	9
CATHODE		
Electric collector	Stainless steel 316 frame + carbon fibers mesh	Isostatic graphite plate (Grade 2114-45)
Electrode	Carbon nanofibers doped with iron nanoparticles	RVG 2000 MERSEN Carbon Felt
Electrode thickness (mm)	0.6	4.6
Compartment thickness (mm)	8.7	9
SALINE COMPARTMENT		
Compartment thickness (mm)	8.7	9
ION EXCHANGE MEMBRANES		
Anionic membrane		Neosepta AMX
Electric resistance (Ω·cm ²)*		2.4
Permselectivity (%)**		>93
Thickness (μm)*		0.14
Cationic membrane		Neosepta CMX
Electric resistance (Ω·cm ²)*		3.0
Permselectivity (%)**		>90
Thickness (μm)*		0.17
OPERATIONAL CONDITIONS		
Operation mode	Batch (3 streams)	Batch (3 streams)
Flow rate (mL·min ⁻¹)	95	95
Temperature (°C)	25–30°C	25–30°C
External load (Ω)	2.5	2.5
STREAMS		
Anolyte	FWM + 2.5 g/L Sodium Acetate	FWM + 1.65 g·L ⁻¹ Sodium Acetate
Catholyte	0.1 M PBS	0.06 M K ₃ Fe(CN) ₆
Saline stream	NaCl	NaCl
TANKS		
Anolyte Volume (mL)	2,500	2,000
Catholyte Volume (mL)	2,500	2,000
Saline Volume (mL)	500	370
Rate V _{an} :V _{saline} :V _{catholyte}	5:1:5	5:1:5
START-UP OPERATION		
Initial inoculum	Electroactive biofilm from an operating MFC	Pure culture <i>Geobacter sulfurreducens</i>
Period (hours)	158	140

*Equilibrated with 0.5N-NaCl solution, at 25°C (data provided by the manufacturer).

**Measured at the laboratory. Membrane equilibrated with 0.1M NaCl and 0.5M NaCl solutions.

neutral pH (Harnisch et al., 2009). Activated carbons, carbon fibers, carbon black and graphene are also use on ORR due to their tuneable surface properties and high surface (Yuan et al.,

2016). More recently, air diffusion cathodes using nanofibers doped with transition metal (Bosch-Jimenez et al., 2017) has been proposed for microbial fuel cells.

Despite the extensive use of oxygen as electron acceptor in METs, the proof of concept of MDC was developed using a ferricyanide catholyte (i.e. Fe(CN)₆³⁻ + 1e⁻ → Fe(CN)₆⁴⁻, E⁰ = 0.36 V) (Cao et al., 2009). Salt removal up to 94%, and energy production of 2 W·m⁻² were achieved, thus increasing significantly the performance of the system compared to that when using ORR as cathodic reaction. Nevertheless, due to high cost of reagents, the use of ferro-ferricyanide catholyte (or other redox mediators/compounds) would be only feasible from a technical point of view in MDCs if: (i) the redox mediator is low cost or (ii) an easy and cheap strategy is developed for regeneration of catholyte solution once depleted.

This work presents the results obtained in parallel in two laboratories (LEITAT and IMDEA Water) for the development of MDC technology for low-energy drinking water production. Similar MDC configurations and experimental methodology have been implemented in both locations in order to compare two different approaches:

- MDC operating using oxygen reduction as cathodic reaction.
- MDC operating using the ferro-ferricyanide redox couple as cathodic reaction.

For the first approach, an air diffusion cathode made of carbon nanofibers and iron nanoparticle as catalyst (produced by electrospinning and pyrolysis) was developed as suitable low-cost electrode for environmental applications (i.e., no use of Pt as catalyst).

In the second approach, a ferro-ferricyanide redox catholyte was studied as an alternative to oxygen reduction, in order to enhance the available potential in the MDC and allow for an improved performance.

Finally, salt removal (SR), nominal desalination rate (NDR), current efficiency, specific energy production (SEP), COD removal rate (COD_{rate}), coulombic efficiency (CE), total circulated charge (Q), and water transport are discussed to compare the pros and cons of the aforementioned MDC approaches.

MATERIALS AND METHODS

Microbial Desalination Cell Set Up

Table 1 shows the main features for both MDCs used in this study. The laboratory MDCs consisted of a three-compartment compact stack design with neoprene gaskets for a hermetical seal (see Figure 1). Graphite felt RVG2000 (MERSEN) and UDCF (SGL) were used as anode electrodes, and isostatic graphite (Grade 2114-45, MERSEN) and stainless steel AISI 316 as anode electric collectors. In the first approach, a novel air diffusion cathode using carbon nanofibers with iron nanoparticles as catalyst was implemented (see section Start-up protocol), and metal frame -stainless steel frame with UDCFs mesh (SGL) as electric collector—was used in the cathodic compartment. For the second approach (i.e., ferro-ferricyanide redox MDC), the materials were the same of the anode compartment. Finally, two

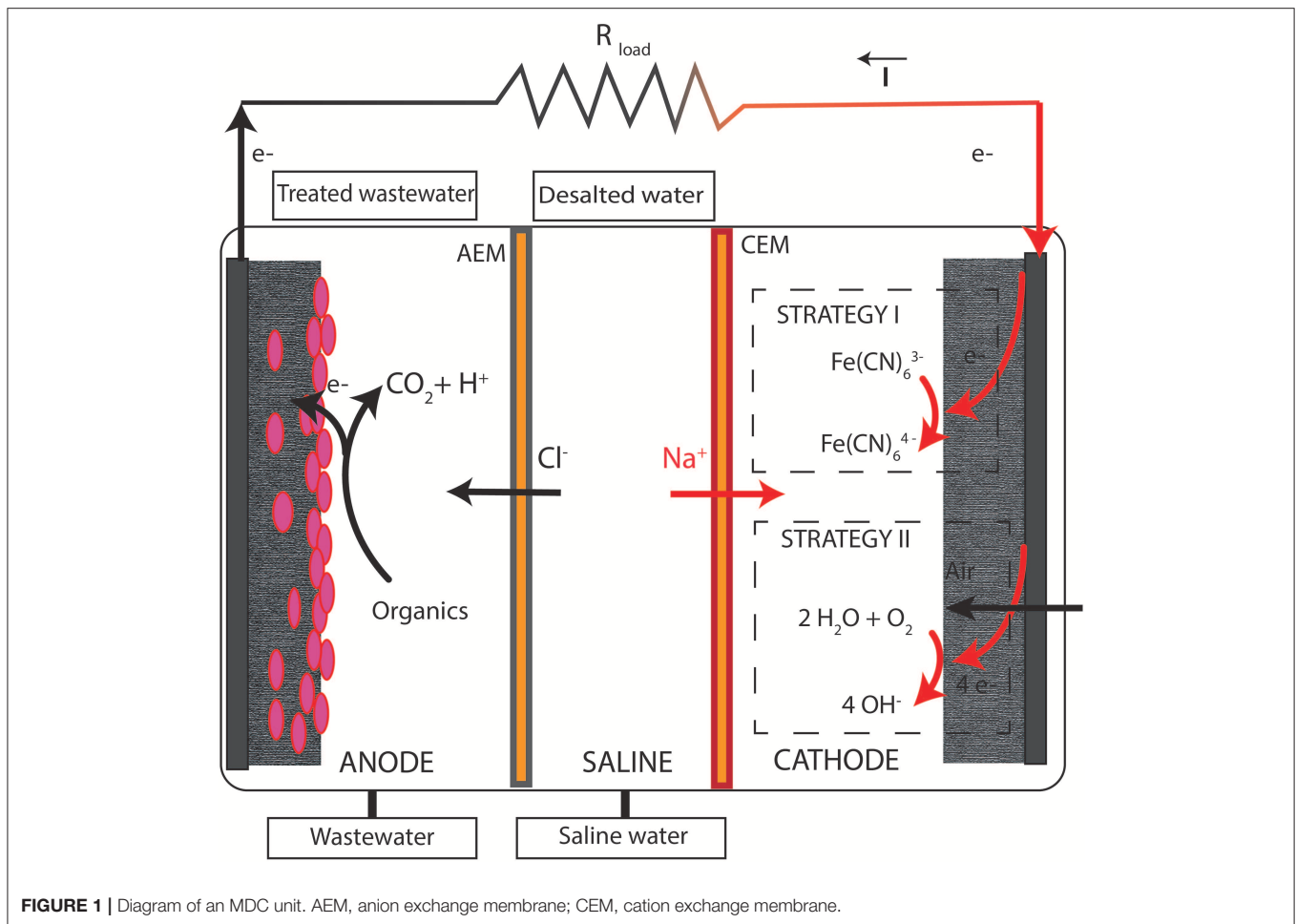


FIGURE 1 | Diagram of an MDC unit. AEM, anion exchange membrane; CEM, cation exchange membrane.

stainless steel end plates were used to close the cell on both ends with a Torque of 10 and 6 N·m for the liquid and air cathode MDCs, respectively.

Figure 2 depicts the diagram of the MDC experimental setup at IMDEA Water and LEITAT facilities (see pictures in **Supplementary Figure 1**). In both cases, the systems were operated in batch mode with recirculation at flow rate of $75 \text{ mL}\cdot\text{min}^{-1}$ (for all streams), and in a temperature-controlled room at 30°C .

The anolyte solution used at LEITAT consisted of a solution containing $0.45 \text{ g}\cdot\text{L}^{-1}$ NaCl, $0.165 \text{ g}\cdot\text{L}^{-1}$ $\text{MgCl}_2\cdot 6\text{H}_2\text{O}$, $0.0136 \text{ g}\cdot\text{L}^{-1}$ CaCl_2 , $0.0153 \text{ g}\cdot\text{L}^{-1}$ Mg_2SO_4 , $8.4 \text{ g}\cdot\text{L}^{-1}$ NaHCO_3 , $0.128 \text{ g}\cdot\text{L}^{-1}$ KH_2PO_4 , $0.925 \text{ mL}\cdot\text{L}^{-1}$ of NH_4Cl 1 M solution, $1 \text{ mL}\cdot\text{L}^{-1}$ of trace element solution and $0.5 \text{ mL}\cdot\text{L}^{-1}$ of Wolfe's vitamins solution, and 20 mM sodium acetate as organic substrate. The catholyte solution consisted of 100 mM Phosphate Buffered Solution (PBS). Saline media was prepared by dissolving $5 \text{ g}\cdot\text{L}^{-1}$ NaCl for brackish water solution and $35 \text{ g}\cdot\text{L}^{-1}$ NaCl for seawater solution.

Similarly, the anolyte solution used at IMDEA Water consisted of fresh water media (FWM) containing $0.1 \text{ g}\cdot\text{L}^{-1}$, KCl, $2.5 \text{ g}\cdot\text{L}^{-1}$ NaHCO_3 , $0.6 \text{ g}\cdot\text{L}^{-1}$ KH_2PO_4 , $0.5 \text{ g}\cdot\text{L}^{-1}$ NH_4Cl , $10 \text{ mL}\cdot\text{L}^{-1}$ of trace element solution and $1 \text{ mL}\cdot\text{L}^{-1}$ of

Wolfe's vitamins solution and 20 mM sodium acetate as organic substrate. The catholyte solution consisted of a $\text{K}_3\text{Fe}(\text{CN})_6$ 100 mM solution. Saline media was prepared by dissolving $5 \text{ g}\cdot\text{L}^{-1}$ NaCl for brackish water solution and $35 \text{ g}\cdot\text{L}^{-1}$ NaCl for seawater solution.

Air Diffusion Cathode

Air cathode was composed of three parts as depicted in **Figure 3**: (i) an external membrane (high density polyethylene fibers textile), impermeable to water and permeable to oxygen; (ii) a conductive material, in this case carbon nanofibers with iron nanoparticles to allow ORR; and (iii) an internal semipermeable membrane (treated high density polyethylene fibers textile) to allow proton exchange.

Start-Up Protocol

A previously reported start-up procedure was followed for both MDCs under study (Borjas et al., 2017). The anolyte, saline, and catholyte streams were firstly sterilized and recirculated through the lab-MDCs. Then, 200 mL of inoculum containing electrogenic bacteria was introduced in the anodic chamber of the MDCs by recirculation with a peristaltic pump.

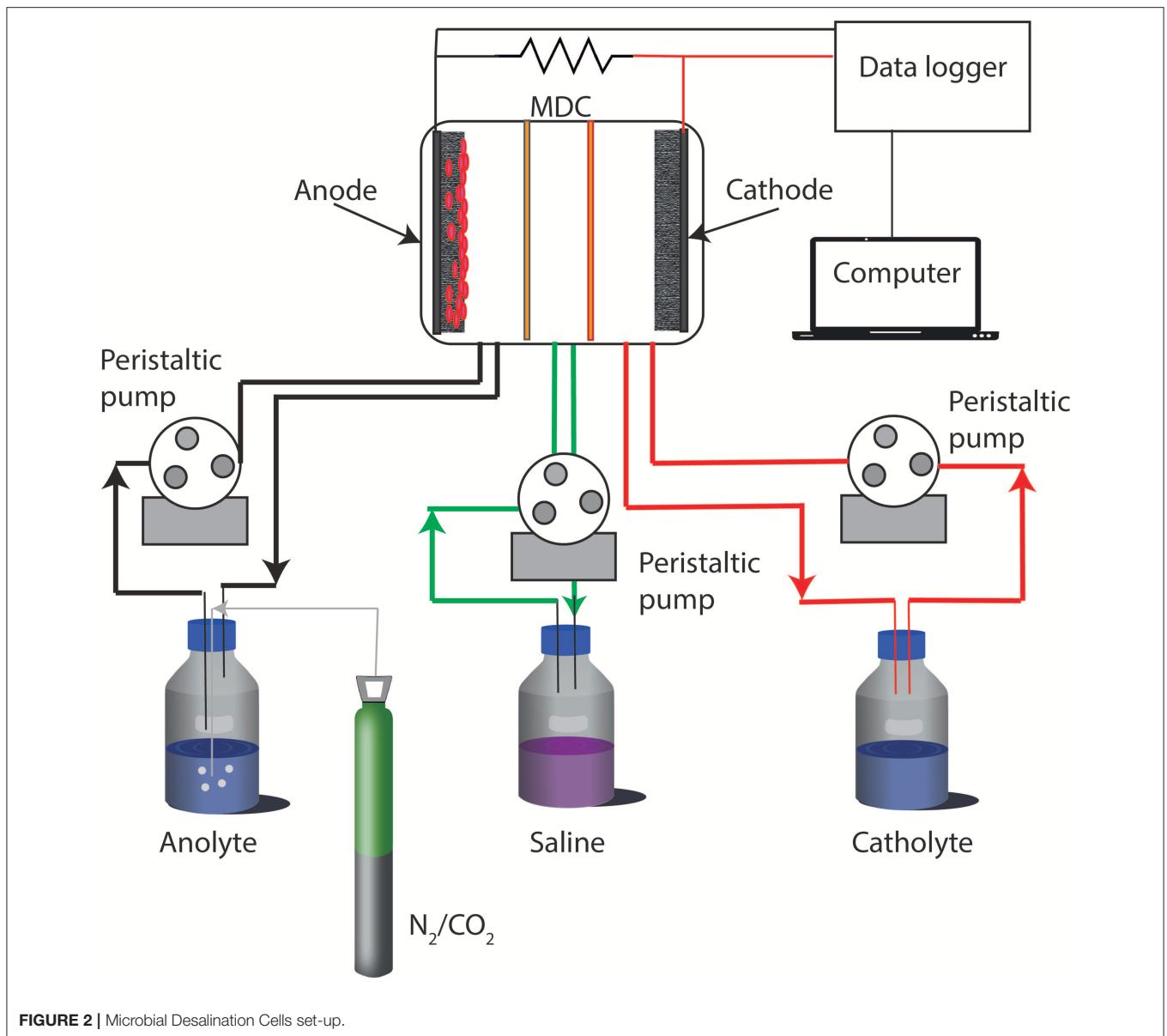


FIGURE 2 | Microbial Desalination Cells set-up.

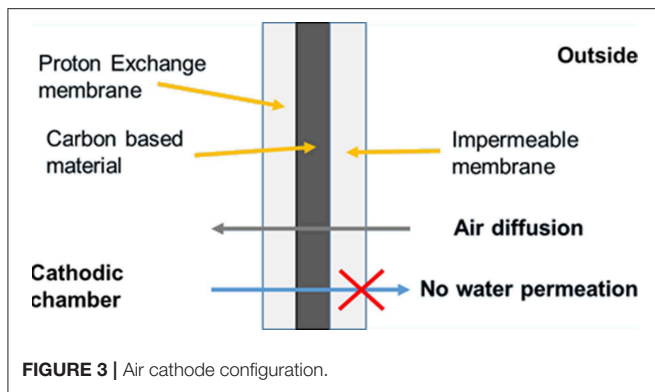
For the air cathode MDC approach, as initial inoculum for start-up, an anodic-electroactive mixed culture from a long term (>3 years) operating Microbial Fuel Cell (MFC) was employed. Initial microbial population content, characterized by MiSeq Illumina platform, accounted for a mixture of Bacteroidetes (6.7%), Firmicutes (3.1%), Proteobacteria (65.9%), Spirochaetes (4.8%), Thermotogae (2.8%), and Verrucomicrobia (9.0%). A selective pressure through a redox potential gradient was applied to the anode in order to promote the growth and attachment of electroactive bacteria onto the electrode. Anode was properly inoculated when current density achieved values higher than $0.15 \text{ mA}\cdot\text{cm}^{-2}$. After that, it was transferred to the MDC.

In the case of the ferro-ferricyanide redox MDC, a pure culture of *Geobacter sulfurreducens* (strain DL1) was used as

inoculum. Exponential-phase culture ($\text{OD}_{600\text{nm}} = 0.4$) was used for the inoculation into the anode compartment in the start-up protocol.

After inoculation of the anodes, the peristaltic pump was switched off overnight, allowing the microorganism to start growing on the anode surface (i.e., graphite felt). After incubation, the pumps were switched on to recirculate the anolyte, catholyte, and saline solutions through the system.

Once the bioanode was considered stable (i.e., no significant variation of electric current), the first desalination cycle was performed with newly-prepared solutions to ensure reproducibility among subsequent desalination cycles. The desalination cycles were finished when the conductivity of the saline tank was below of $1 \text{ mS}\cdot\text{cm}^{-1}$, as this threshold could be



considered as optimum value for water quality (Council Directive 75/440/EEC, 1975).

Calculations

The following equations were used to determine the main parameters of the MDCs performance. Current density, j ($\text{mA}\cdot\text{cm}^{-2}$), was calculated by:

$$j = \frac{I}{A_m} \quad (1)$$

where I is the electric current (mA) and A_m is the effective electrode surface area (cm^2).

Salt removal, SR (%), refers to the percentage of NaCl removed during every desalination cycle, and it can be expressed by:

$$SR = \frac{c_s^i - c_s^f}{c_s^i} \quad (2)$$

where c_s^i and c_s^f represent the initial and final molar concentrations of salt in the saline tank ($\text{mol}\cdot\text{m}^{-3}$), respectively.

Nominal Desalination rate, NDR ($\text{L}\cdot\text{m}^{-2}\cdot\text{h}^{-1}$), refers to the normalized amount of fresh water per square meter of membrane during every desalination cycle, and it can be expressed by:

$$NDR = \frac{Q_t}{A_m \cdot t_d} \quad (3)$$

where, t_d is the desalination time (h) (i.e., conductivity of saline tank below of $1\text{ mS}\cdot\text{cm}^{-1}$), and Q_t is the volume of desalinated water (L).

Specific energy production, SEP ($\text{kWh}\cdot\text{m}^{-3}$), defines the energy produced by the MDC per cubic meter of fresh water, and it can be expressed by:

$$SEP = \frac{1}{Q_t} \int E_{\text{cell}} I(t) dt \quad (4)$$

where E_{cell} is the electric potential provided by the MDC device (V).

Current efficiency, η_c (%), defines the percentage of the total charge associated to the salt removed from the saline

compartment to the amount of electric charge transferred across the membranes (ECT, $\text{C}\cdot\text{m}^{-3}$) over a complete process of desalination. η_c and ECT were calculated using Equations 5 and 6, respectively.

$$\eta_c = \frac{\nu z F (c_s^i - c_s^f)}{\text{ECT}} \quad (5)$$

$$\text{ECT} = \frac{1}{Q_t} \int I(t) dt \quad (6)$$

where, ν and z represent the stoichiometric coefficient and the valence of the salt ions, respectively, and F is the Faraday constant ($96,485\text{ C}\cdot\text{mol}^{-1}$).

Coulombic efficiency, η_{Cb} , is defined as the ratio of total electric charge transferred to the anode from the consumed organic substrate and it can be expressed by:

$$\eta_{Cb} = \frac{M \int I(t) dt}{F \cdot b \cdot Q_{An} \cdot \Delta\text{COD}} \quad (7)$$

where M is the molecular weight of oxygen ($32\text{ g}\cdot\text{mol}^{-1}$), b is the number of electrons exchanged per mole of oxygen ($b = 4$), Q_{An} is the volume of the anolyte tank (L), and ΔCOD is the change in chemical oxygen demand (COD) for the experiment ($\text{mg O}_2\cdot\text{L}^{-1}$).

COD removal rate, COD_{rate} ($\text{kg}\cdot\text{m}^{-3}\cdot\text{day}^{-1}$), was calculated using the next expression:

$$\text{COD}_{rate} = \frac{\Delta\text{COD}}{V_A t_d} \quad (8)$$

where V_A is the volume of liquid in the anode compartment (m^3).

The total circulated charge, Q (Coulomb), was calculated according to Equation 9:

$$Q = \int I(t) dt \times t_d \quad (9)$$

RESULTS AND DISCUSSION

Both MDC strategies (i.e., ORR as cathodic reaction, ferro-ferricyanide redox system as cathodic reaction) were compared using laboratory-scale MDCs with 100 cm^2 of cross section (or geometric electrode surface). Experimental results are showed in **Figure 4**. Experiments were carried out at two different initial saline concentrations: brackish water range (NaCl $7.5\text{--}10\text{ g}\cdot\text{L}^{-1}$) with an initial electric conductivity of 13.9 and $17.5\text{ mS}\cdot\text{cm}^{-1}$ for ferro-ferricyanide redox and air cathode approach, respectively, and seawater range (NaCl $35\text{ g}\cdot\text{L}^{-1}$), with an initial electric conductivity of 51.5 and $53.3\text{ mS}\cdot\text{cm}^{-1}$ for ferro-ferricyanide redox and air cathode approach. Nominal desalination rate, salt removal, current efficiency and COD removal rate were compared between both strategies to compare the feasibility of MDC technology, understand its limitations, describe its advantages and disadvantages and elucidate which strategy is more convenient for scaling up of the technology in real environments.

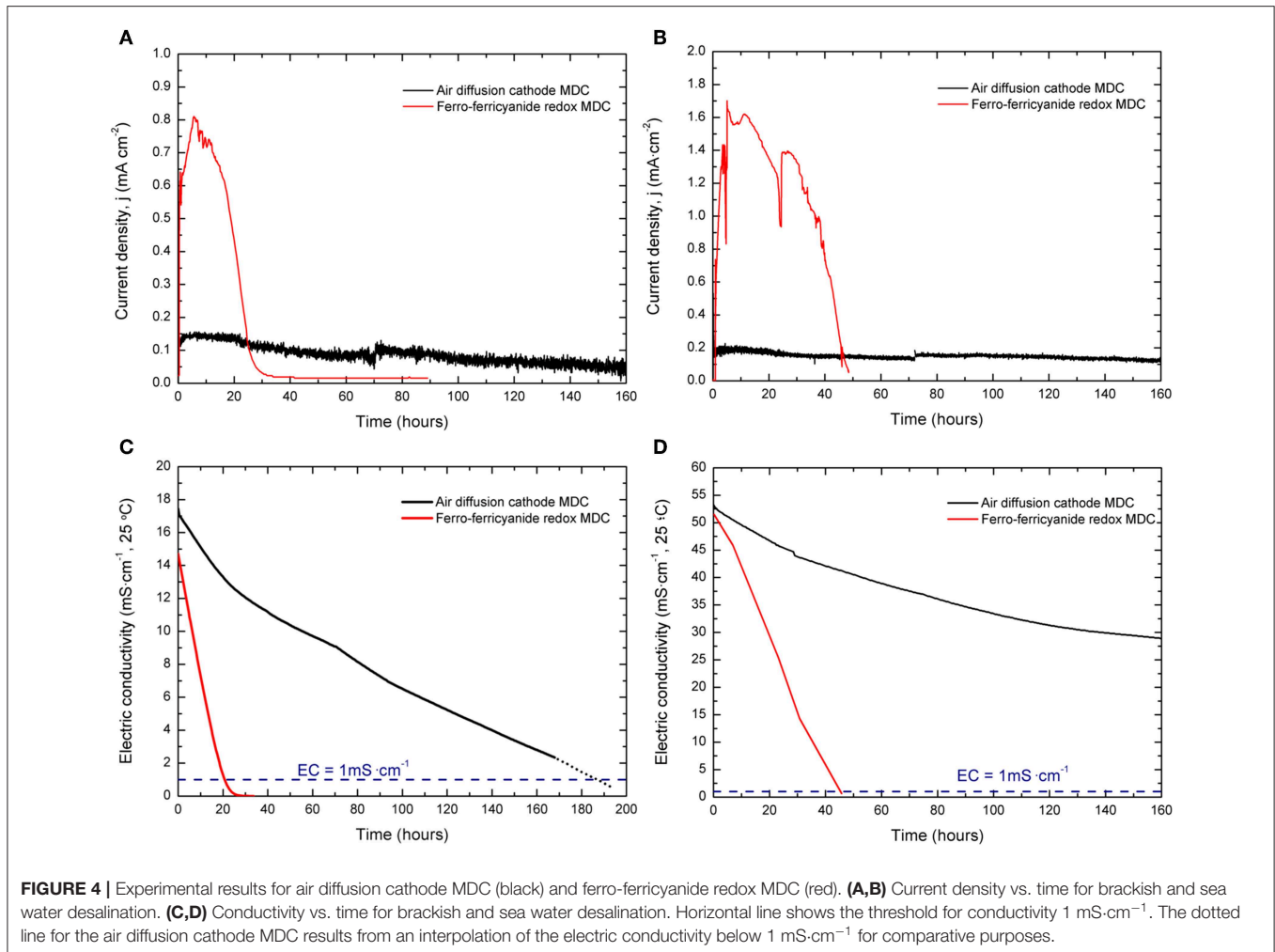


FIGURE 4 | Experimental results for air diffusion cathode MDC (black) and ferro-ferricyanide redox MDC (red). **(A,B)** Current density vs. time for brackish and sea water desalination. **(C,D)** Conductivity vs. time for brackish and sea water desalination. Horizontal line shows the threshold for conductivity 1 mS·cm⁻¹. The dotted line for the air diffusion cathode MDC results from an interpolation of the electric conductivity below 1 mS·cm⁻¹ for comparative purposes.

Brackish Water Desalination

Figure 4A shows the electric current for brackish water desalination experiments using the aforementioned strategies. Maximum current densities for air diffusion and ferro-ferricyanide cathode were 0.14 and 0.81 mA·cm⁻², respectively. As both devices used the same external load (2.5 Ω) and analogous anodes and configurations, the higher electric current obtained when using the ferro-ferricyanide redox MDC may be directly related to the cathode reaction, which provide higher available potential to drive the desalination process.

In general, it could be stated that from the thermodynamic point of view, the available potential in the MDC to perform the desalination process is higher when oxygen reduction is used in the cathode [$E_{MDC}^0 = E_{cathode}^0 - E_{anode}^0 = 0.81 \text{ V} - (-0.3 \text{ V}) = 1.11 \text{ V}$]. However, oxygen reduction reaction provides less potential than expected in the range of current densities (i.e., 0.2–1.5 mA·cm⁻²) used for desalination in MDC systems, and it is mainly related to slow kinetics associated to this reaction at pH = 7 (or neutral), that is common in microbial electrochemical systems. On the other hand, regardless the lower thermodynamic potential when ferri-ferricyanide reduction is used in the

cathode compartment [$E_{MDC}^0 = 0.36 - (-0.3 \text{ V}) = 0.66 \text{ V}$], fast kinetic provides more available potential when implemented in MDC systems. Thus, the lower potential available is the reason behind the poor desalination performance when oxygen reduction is used as cathodic reaction.

Figure 4C shows the electric conductivity for brackish water desalination using the aforementioned strategies. As the electric current is also directly related to migration of ion species, the desalination time (i.e., time required to achieve the threshold conductivity of 1 mS·cm⁻¹) for the ferro-ferricyanide redox MDC is lower compared to the air cathode MDC.

As shown in Figure 4C, the current density in ferro-ferricyanide redox cathode experiment decreased from 0.81 mA·cm⁻² in 16 h to 0.08 mA·cm⁻². This decrease is attributable to the drop in conductivity of the salinity compartment from 14 to 0.56 mS·cm⁻¹. In the case of the air cathode experiment, the current density dropped from 0.14 to 0.08 mA·cm⁻² in 160 h, decreasing the conductivity in the saline compartment from 16 to 2.4 mS·cm⁻¹. The decrease of current density in both MDC cases could be linked to the increase of the internal resistance of the MDC, as electric conductivity decreases during

TABLE 2 | Initial and final salinity, salt removal, desalination time, current efficiency, nominal desalination rate, COD removal rate, anode coulombic efficiency, specific energy production, total circulated charge and volume variation for air diffusion cathode and ferro-ferricyanide redox MDC experiments for brackish water desalination.

	Air-diffusion cathode MDC	Ferro-ferricyanide redox MDC
Initial salinity (g·L ⁻¹)	10.7	7.3
Final salinity (g·L ⁻¹)	0.5	0.5
Salt removal (%)	93.6	93.3
Desalination time (h)	205	23
NDR (L·m ⁻² ·h ⁻¹)*	0.17**	1.5
Current efficiency (%)	162	81.1
COD removal rate (kg COD·m ⁻³ ·day ⁻¹)***	0.94	7.14
Coulombic efficiency (%)	6.5	91.0
Specific energy production (kWh·m ⁻³)	0.017	0.7
Total circulated charge (Q)	5086	5165
Volume variation (%)	-36.0	-8.1

*Calculated considering the final volume of saline tank.

**Extrapolated from experimental results.

***Considering the volume of anolyte compartment.

the experiments. These observations are in accordance with previous MDC behavior operating in batch mode (Borjas et al., 2017).

It is worthwhile to mention that the air diffusion cathode developed in this study (Fe-doped C-NF) displayed higher current densities compared with analogous studies in the literature (in the range of 0.084 mA·cm⁻², using Pt coated air diffusion cathode when desalinating 10 g·L⁻¹ brackish water) (Jafary et al., 2018). **Table 2** shows the main experimental performance parameters for brackish water desalination using both cathodic reactions

For both desalination cycles the salt removal exceeded 90%, indicating proper performance of both MDCs as desalination devices. Regarding nominal desalination rate (NDR), the ferro-ferricyanide redox MDC was able to produce almost six times higher amount of desalinated water (1.54 L·m⁻²·h⁻¹) compared to that of the air diffusion cathode MDC (0.17 L·m⁻²·h⁻¹). Current efficiencies were 162% and 81.1% for air diffusion cathode and ferro-ferricyanide redox MDC, respectively. As current efficiency determines the rate of current that is used for ion migration, values above 100% means that an additional transport phenomena occurred during the experiment, i.e., diffusion from saline to adjacent compartments.

From the point of view of waste water treatment, COD removal rates for both air diffusion cathode and ferro-ferricyanide redox MDCs were 0.94 and 7.14 kg COD·m⁻³·day⁻¹. This parameter is related to the current density and desalination performance, as consumption of COD provides the electric current to drive the desalination process. The coulombic efficiency decayed at longer desalination times (t_d), as it is the case of the air diffusion cathode MDC experiment. This fact may be due to a competition between electrogenic and

TABLE 3 | Initial and final salinity, salt removal, desalination time, current efficiency, nominal desalination rate, COD removal rate, anode coulombic efficiency, specific energy production, total circulated charge and volume variation for air diffusion cathode and ferro-ferricyanide redox MDC experiments for sea water desalination.

	Air-diffusion cathode MDC**	Ferro-ferricyanide redox MDC
Initial salinity (g·L ⁻¹)	33.5	35.0
Final salinity (g·L ⁻¹)	17.4	0.5
Salt removal (%)	48.2	98.6
Desalination time (h)	-	43
NDR (L·m ⁻² ·h ⁻¹)*	0.14	0.7
Current efficiency (%)	145	108
COD removal rate (kg COD·m ⁻³ ·day ⁻¹)	1.07	19.7
Coulombic efficiency (%)	10.3	61.0
Specific Energy Production (kWh·m ⁻³)	0.055	5.4
Total circulated charge (Q)	8,994	19,354
Volume variation (%)	-2	-19

*Calculated considering the final volume of saline tank.

**Calculated for partial desalination.

anaerobic microorganism since the latter do not contribute to electric current generation.

Specific energy production (SEP) was 0.02 and 0.8 kWh·m⁻³ for air diffusion cathode and ferro-ferricyanide redox MDC, respectively. This fact indicates that in both cases it is possible to generate a significant amount of electric energy simultaneously with desalinated water production and waste water treatment, as reported in the literature (Sophia et al., 2016; Sevda and Abu-Reesh, 2018).

Finally, the water transport was measured by determining the change in the final volume of the saline tank. Water transport across membranes was remarkable for air diffusion cathode MDC experiment, accounting for 36% decrease (v/v). In the case of the ferro-ferricyanide redox MDC, the volume decrease remained below 10% (v/v). Water transport may be attributable to osmosis and/or electrosomosis phenomena (i.e., water transport due to electric charge). As the desalination conditions were similar for both cases (i.e., electric charge to perform desalination, see **Table 2**), the water transport could be attributed to osmosis. In this sense, for a similar water flux due to osmosis, a higher desalination time allows for a higher osmosis water transport, as indicated in **Table 2** for the air diffusion cathode experiment.

Seawater Desalination

Figure 4B shows the electric current for sea water desalination experiments. In this case, air diffusion cathode MDC and ferro-ferricyanide redox MDC experiments achieved maximum current densities of 0.20 and 1.70 mA·cm⁻², respectively. Similarly to the previously discussed results, the current density for ferro-ferricyanide redox MDC decreased from 1.7 to 0.1 mA·cm⁻² in 48 h due to the drop in the conductivity of the salinity compartment (from 50 to 0.6 mS·cm⁻¹) as depicted in **Figure 4B**. For the air cathode MDC experiment, the current

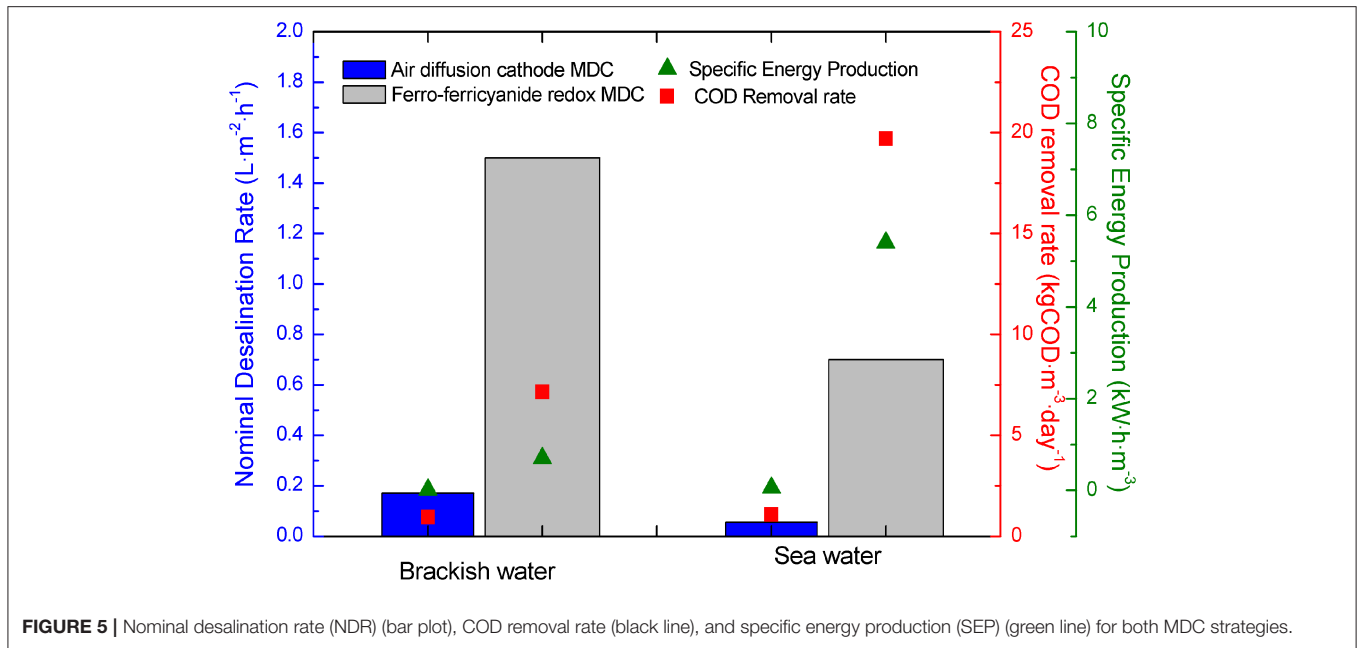


FIGURE 5 | Nominal desalination rate (NDR) (bar plot), COD removal rate (black line), and specific energy production (SEP) (green line) for both MDC strategies.

density dropped from 0.2 to 0.12 mA·cm⁻² in 160 h, while decreasing the salinity from 51 to 28 mS·cm⁻¹.

Figure 4D shows the electric conductivity for sea water desalination. In this case, the air diffusion cathode MDC was not able to accomplish complete desalination (i.e., electric conductivity below threshold value of 1 mS·cm⁻¹). **Table 3** shows the main experimental performance parameters for the sea water desalination experiment.

It is important to note that for the air diffusion cathode MDC, the salt removal was around 20%, indicating that only partial desalination was achieved. The partial desalination has been also reported in the literature with similar MDC configuration using oxygen reduction as cathode reaction (decrease of 58 to 22 mS·cm⁻¹, salt removal 50%) (Zhang and He, 2015; Moruno et al., 2018). This effect could be attributed to the low available potential to drive the migration of the ions. When the electric conductivity increased in the anodic/cathode chamber due to the migration of the ions from the saline compartment during the desalination cycle, back-diffusion transport of salt started to be significant, and eventually this ionic transport was equal to the ionic transport due to migration. This resulted in a zero net balance of salinity in the saline compartment (Ping et al., 2016). This effect could be observed in **Figure 4D** from the asymptotic trend of the electric conductivity for the air diffusion cathode MDC (28 mS·cm⁻¹). In the case of ferro-ferricyanide redox MDC, complete desalination was achieved, being the desalination time 43 h (t_d).

NDR values were 0.14 L·m⁻²·h⁻¹ for partial desalination (air diffusion cathode MDC), and 0.7 L·m⁻²·h⁻¹ for the ferro-ferricyanide redox MDC. This latter value is slightly higher compared to analogs MDC systems operating with ferro-ferricyanide catholyte (Cao et al., 2009; Luo et al., 2012; Kalleary et al., 2014; Chen et al., 2015) likely due to recirculation, thickness of the saline compartment and low external load value. Current

efficiencies were above 100%, indicating higher ion migration which could be attributed to the electric current achieved. Thus, diffusion from saline compartment to adjacent compartments was more significant for sea water desalination compared to brackish water desalination (see **Tables 2, 3**). Regarding volume variation, it could be attributed to osmotic processes due to the longer duration in the air cathode MDC configuration as well as different initial conductivity in catholyte solutions in both configurations.

Figure 5 summarizes the main experimental results for both MDC strategies for brackish and sea water desalination. As stated, NDR was higher for brackish and sea water when the ferro-ferricyanide redox MDC was used, and only complete desalination could be achieved using air diffusion cathode MDC for brackish water desalination (i.e., partial desalination for sea water). From the point of view of COD removal rate, desalination of sea water increased the waste water capacity of the MDC, and this effect was related to the increase in the generation of electric current. Similarly, specific energy production (SEP) was higher for seawater desalination compared to brackish water's.

From the point of view of real application, brackish water desalination can be accomplished by both strategies. As oxygen is a simple and available reagent, air diffusion cathode MDC is more suitable for brackish water desalination, but water production (i.e., NDR) should be maximized by complete optimization of the system. In the case of sea water desalination, only ferro-ferricyanide redox MDC could achieve complete desalination, so air diffusion MDC strategy could be adopted as a suitable approach for pre-desalination step applications (for example, coupled to a RO conventional plant Elmekawy et al., 2014). Obviously, even if ferro-ferricyanide redox catholyte allows the increase of the desalination efficiency, waste water treatment, fresh water, and energy production in the MDC device, it should

be regenerated when depleted due to the high costs of reagents, as previously discussed in the literature Cao et al., 2009. For this reason, low-cost and effective strategies for regeneration of the redox mediator catholyte need to be explored in next studies, for instance, using renewable energy (i.e., photovoltaic, wind energy) or other microbial electrochemical processes (i.e., biocathodes).

Finally, the experimental results of this study have been obtained in two different laboratories, with systematic experimental approach and in close collaboration. The consistent and reproducible experimental results shall help the further development of MDC technology and to speed up their scaling-up for operation in real environments.

CONCLUSIONS

Microbial Desalination Cell constitutes an innovative technology where microbial fuel cells and electro dialysis merge in the same device for obtaining fresh water with no energy-associated costs, while treating wastewater and producing energy. One of the main limitations for MDC technology is the low available potential for desalination when oxygen reduction is used as cathodic reaction, as partial desalination is obtained when sea water is used as feed stream. The ferro-ferricyanide redox MDC strategy has been proposed in the literature in order to enhance the performance of MDC technology and provide total desalination of sea water. Two analogous MDC experimental setups with different cathode strategy (air diffusion and ferro-ferricyanide redox) allow to compare the desalination performance of both systems, and to understand the main limitations for the technology development. Air cathode approach may be suitable for brackish water desalination, even though nominal desalination rates are near one order of magnitude lower than those obtained using a ferro-ferricyanide redox mediator. Seawater desalination could be better addressed by a ferro-ferricyanide redox MDC; however, catholyte regeneration routes should be explored to reduce costs and allow for low-cost and efficient desalination. A compromise between MDC performance and costs should be made for further upscaling and application in real environments. Finally, the

proposed methodology could be an interesting approach for inter laboratory collaboration for further MDC studies.

DATA AVAILABILITY STATEMENT

The datasets generated for this study are available on request to the corresponding author.

AUTHOR CONTRIBUTIONS

MR-M performed the experiments related to ferro/ferricyanide catholyte. PR helped in the experimental stage, collected and organized all the experimental data, and wrote the manuscript. MA and PB-J performed the manufacturing process and experiments related to air diffusion cathode. EB also participated in the air-cathode design and supervised the experimental work. PZ coordinated and supervised the inter-laboratory experimental work and corrected the manuscript. VM and FR supervised the experimental work. JO and AE-N designed experiments related to ferro/ferricyanide catholyte and critically reviewed the manuscript. All authors participated in manuscript writing.

FUNDING

Project MIDES – H2020 has received funding from the European Union's Horizon 2020 research and innovation programme under grant agreement No. 685793. MR-M acknowledges the financial support of Consejería de Educación e Investigación de la Comunidad de Madrid and Fondo Social Europeo (Ref: PEJD-2018-PRE/AMB-8721). JO acknowledges the financial support of Agencia Estatal de Investigación (AEI) and Fondo Europeo de Desarrollo Regional (FEDER) (Proyecto BioDES, CTM2015-74695-JIN).

SUPPLEMENTARY MATERIAL

The Supplementary Material for this article can be found online at: <https://www.frontiersin.org/articles/10.3389/fenrg.2019.00135/full#supplementary-material>

REFERENCES

- Badiuzzaman, P., McLaughlin, E., and McCauley, D. (2017). Substituting freshwater: can ocean desalination and water recycling capacities substitute for groundwater depletion in California? *J. Environ. Manage.* 203, 123–135. doi: 10.1016/j.jenvman.2017.06.051
- Bashyam, R., and Zelenay, P. (2006). A class of non-precious metal composite catalysts for fuel cells. *Nature* 443, 63–66. doi: 10.1038/nature05118
- Borjas, Z., Esteve-Núñez, A., and Ortiz, J. M. (2017). Strategies for merging microbial fuel cell technologies in water desalination processes: start-up protocol and desalination efficiency assessment. *J. Power Sources* 356, 519–528. doi: 10.1016/j.jpowsour.2017.02.052
- Bosch-Jimenez, P., Martínez-Crespiera, S., Amantia, D., Della Pirriera, M., Forns, I., Shechter, R., et al. (2017). Non-precious metal doped carbon nanofiber air-cathode for Microbial Fuel Cells application: oxygen reduction reaction characterization and long-term validation. *Electrochim. Acta* 228, 380–388. doi: 10.1016/j.electacta.2016.12.175
- Cao, X., Huang, X., Liang, P., Xiao, K., Zhou, Y., Zhang, X., et al. (2009). A new method for water desalination using microbial desalination cells. *Environ. Sci. Technol.* 43, 7148–7152. doi: 10.1021/es901950j
- Chen, S., Luo, H., Hou, Y., Liu, G., Zhang, R., and Qin, B. (2015). Comparison of the removal of monovalent and divalent cations in the microbial desalination cell. *Front. Environ. Sci. Eng.* 9, 317–323. doi: 10.1007/s11783-013-0596-y
- Chen, X., Liang, P., Wei, Z., Zhang, X., and Huang, X. (2012). Sustainable water desalination and electricity generation in a separator coupled stacked microbial desalination cell with buffer free electrolyte circulation. *Bioresour. Technol.* 119, 88–93. doi: 10.1016/j.biortech.2012.05.135
- Chen, X., Xia, X., Liang, P., Cao, X., Sun, H., and Huang, X. (2011). Stacked microbial desalination cells to enhance water desalination efficiency. *Environ. Sci. Technol.* 45, 2465–2470. doi: 10.1021/es103406m
- Chowdhury, A. H., Scanlon, B. R., Reedy, R. C., and Young, S. (2018). Fingerprinting groundwater salinity sources in the Gulf Coast Aquifer System, USA. *Hydrogeol. J.* 26, 197–213. doi: 10.1007/s10040-017-1619-8

- Council Directive 75/440/EEC (1975). Council Directive 75/440/EEC of 16 June 1975 concerning the quality required of surface water intended for the abstraction of drinking water in the Member States.
- Elmekawy, A., Hegab, H. M., and Pant, D. (2014). The near-future integration of microbial desalination cells with reverse osmosis technology. *Energy Environ. Sci.* 7, 3921–3933. doi: 10.1039/C4EE02208D
- Freguia, S., Rabaey, K., Yuan, Z., and Keller, J. (2007). Non-catalyzed cathodic oxygen reduction at graphite granules in microbial fuel cells. *Electrochim. Acta* 53, 598–603. doi: 10.1016/j.electacta.2007.07.037
- Freguia, S., Rabaey, K., Yuan, Z., and Keller, J. (2008). Sequential anode-cathode configuration improves cathodic oxygen reduction and effluent quality of microbial fuel cells. *Water Res.* 42, 1387–1396. doi: 10.1016/j.watres.2007.10.007
- Ge, X., Sumboja, A., Wu, D., An, T., Li, B., Goh, F. W. T., et al. (2015). Oxygen reduction in alkaline media: from mechanisms to recent advances of catalysts. *ACS Catal.* 5, 4643–4667. doi: 10.1021/acscatal.5b00524
- Ge, Z., Dosoretz, C. G., and He, Z. (2014). Effects of number of cell pairs on the performance of microbial desalination cells. *Desalination* 341, 101–106. doi: 10.1016/j.desal.2014.02.029
- Harnisch, F., Wirth, S., and Schröder, U. (2009). Effects of substrate and metabolite crossover on the cathodic oxygen reduction reaction in microbial fuel cells: platinum vs. iron(II) phthalocyanine based electrodes. *Electrochem. Commun.* 11, 2253–2256. doi: 10.1016/j.elecom.2009.10.002
- Jacobson, K. S., Drew, D. M., and He, Z. (2011a). Efficient salt removal in a continuously operated upflow microbial desalination cell with an air cathode. *Bioresour. Technol.* 102, 376–380. doi: 10.1016/j.biortech.2010.06.030
- Jacobson, K. S., Drew, D. M., and He, Z. (2011b). Use of a liter-scale microbial desalination cell as a platform to study bioelectrochemical desalination with salt solution or artificial seawater. *Environ. Sci. Technol.* 45, 4652–4657. doi: 10.1021/es200127p
- Jafary, T., Daud, W. R. W., Aljlil, S. A., Ismail, A. F., Al-Mamun, A., Baawain, M. S., et al. (2018). Simultaneous organics, sulphate and salt removal in a microbial desalination cell with an insight into microbial communities. *Desalination* 445, 204–212. doi: 10.1016/j.desal.2018.08.010
- Kalleary, S., Mohammed Abbas, F., Ganesan, A., Meenatchisundaram, S., Srinivasan, B., Packirisamy, A. S. B., et al. (2014). Biodegradation and bioelectricity generation by Microbial Desalination Cell. *Int. Biodeterior. Biodegrad.* 92, 20–25. doi: 10.1016/j.ibiod.2014.04.002
- Kim, Y., and Logan, B. E. (2011). Series assembly of microbial desalination cells containing stacked electrodialysis cells for partial or complete seawater desalination. *Environ. Sci. Technol.* 45, 5840–5845. doi: 10.1021/es200584q
- Lefèvre, M., Proietti, E., Jaouen, F., and Dodelet, J.-P. (2009). Iron-based catalysts with improved oxygen reduction activity in polymer electrolyte fuel cells. *Science* 324, 71–74. doi: 10.1126/science.1170051
- Liu, X.-W., Sun, X.-F., Huang, Y.-X., Sheng, G.-P., Zhou, K., Zeng, R. J., et al. (2010). Nano-structured manganese oxide as a cathodic catalyst for enhanced oxygen reduction in a microbial fuel cell fed with a synthetic wastewater. *Water Res.* 44, 5298–5305. doi: 10.1016/j.watres.2010.06.065
- Lu, M., and Li, S. F. Y. (2012). Cathode reactions and applications in microbial fuel cells: a review. *Crit. Rev. Environ. Sci. Technol.* 42, 2504–2525. doi: 10.1080/10643389.2011.592744
- Luo, H., Xu, P., and Ren, Z. (2012). Long-term performance and characterization of microbial desalination cells in treating domestic wastewater. *Bioresour. Technol.* 120, 187–193. doi: 10.1016/j.biortech.2012.06.054
- MacHarg, J. P., Seacord, T. F., and Sessions, B. (2008). ADC baseline tests reveal trends in membrane performance. *Desalin. Water Reuse* 18, 1–9. Available online at: <http://citeseerx.ist.psu.edu/viewdoc/download?doi=10.1.1.608.2998&rep=rep1&type=pdf>
- Mehanna, M., Saito, T., Yan, J., Hickner, M., Cao, X., Huang, X., et al. (2010). Using microbial desalination cells to reduce water salinity prior to reverse osmosis. *Energy Environ. Sci.* 3, 1114–1120. doi: 10.1039/c002307h
- Moruno, F. L., Rubio, J. E., Santoro, C., Atanassov, P., Cerrato, J. M., and Arges, C. G. (2018). Investigation of patterned and non-patterned poly(2,6-dimethyl 1,4-phenylene) oxide based anion exchange membranes for enhanced desalination and power generation in a microbial desalination cell. *Solid State Ionics* 314, 141–148. doi: 10.1016/j.ssi.2017.11.004
- Ortiz, J. M., Sotoca, J. A., Expósito, E., Gallud, F., García-García, V., Montiel, V., et al. (2005). Brackish water desalination by electrodialysis: batch recirculation operation modeling. *J. Memb. Sci.* 252, 65–75. doi: 10.1016/j.memsci.2004.11.021
- Ping, Q., and He, Z. (2013). Improving the flexibility of microbial desalination cells through spatially decoupling anode and cathode. *Bioresour. Technol.* 144, 304–310. doi: 10.1016/j.biortech.2013.06.117
- Ping, Q., Porat, O., Dosoretz, C. G., and He, Z. (2016). Bioelectricity inhibits back diffusion from the anolyte into the desalinated stream in microbial desalination cells. *Water Res.* 88, 266–273. doi: 10.1016/j.watres.2015.10.018
- Qu, Y., Feng, Y., Wang, X., Liu, J., Lv, J., He, W., et al. (2012). Simultaneous water desalination and electricity generation in a microbial desalination cell with electrolyte recirculation for pH control. *Bioresour. Technol.* 106, 89–94. doi: 10.1016/j.biortech.2011.11.045
- Sevda, S., and Abu-Reesh, I. M. (2018). Improved salt removal and power generation in a cascade of two hydraulically connected up-flow microbial desalination cells. *J. Environ. Sci. Heal. Part A* 53, 326–337. doi: 10.1080/10934529.2017.1400805
- Shaffer, D. L., Werber, J. R., Jaramillo, H., Lin, S., and Elimelech, M. (2014). Forward osmosis: where are we now?. *Desalination* 356, 271–284. doi: 10.1016/j.desal.2014.10.031
- Sharon, H., and Reddy, K. S. (2015). A review of solar energy driven desalination technologies. *Renew. Sustain. Energy Rev.* 41, 1080–1118. doi: 10.1016/j.rser.2014.09.002
- Sophia, A. C., Bhalambal, V. M., Lima, E. C., and Thirunavoukkarasu, M. (2016). Microbial desalination cell technology: contribution to sustainable waste water treatment process, current status and future applications. *J. Environ. Chem. Eng.* 4, 3468–3478. doi: 10.1016/j.jece.2016.07.024
- Talbot, D. (2015). *The World's Largest and Cheapest Reverse-Osmosis Desalination Plant is up and Running in Israel*. MIT Technology Review.
- Vij, V., Sultan, S., Harzandi, A. M., Meena, A., Tiwari, J. N., Lee, W.-G., et al. (2017). Nickel-based electrocatalysts for energy-related applications: oxygen reduction, oxygen evolution, and hydrogen evolution reactions. *ACS Catal.* 7, 7196–7225. doi: 10.1021/acscatal.7b01800
- Wang, P., and Chung, T.-S. (2015). Recent advances in membrane distillation processes: membrane development, configuration design and application exploring. *J. Memb. Sci.* 474, 39–56. doi: 10.1016/j.memsci.2014.09.016
- Wang, Q., Huang, L., Yu, H., Quan, X., Li, Y., Fan, G., et al. (2015). Assessment of five different cathode materials for Co(II) reduction with simultaneous hydrogen evolution in microbial electrolysis cells. *Int. J. Hydrogen Energy* 40, 184–196. doi: 10.1016/j.ijhydene.2014.11.014
- Water Scarcity (2019). *UN Water*. Available online at: <http://www.unwater.org/water-facts/scarcity/> (accessed April 1, 2019).
- Wen, Q., Zhang, H., Chen, Z., Li, Y., Nan, J., and Feng, Y. (2012). Using bacterial catalyst in the cathode of microbial desalination cell to improve wastewater treatment and desalination. *Bioresour. Technol.* 125, 108–113. doi: 10.1016/j.biortech.2012.08.140
- Yuan, H., Abu-Reesh, I. M., and He, Z. (2015). Enhancing desalination and wastewater treatment by coupling microbial desalination cells with forward osmosis. *Chem. Eng. J.* 270, 437–443. doi: 10.1016/j.cej.2015.02.059
- Yuan, H., Hou, Y., Abu-Reesh, I. M., Chen, J., and He, Z. (2016). Oxygen reduction reaction catalysts used in microbial fuel cells for energy-efficient wastewater treatment: a review. *Mater. Horizons* 3, 382–401. doi: 10.1039/C6MH00093B
- Yuan, L., Yang, X., Liang, P., Wang, L., Huang, Z.-H., Wei, J., et al. (2012). Capacitive deionization coupled with microbial fuel cells to desalinate low-concentration salt water. *Bioresour. Technol.* 110, 735–738. doi: 10.1016/j.biortech.2012.01.137
- Zhang, B., and He, Z. (2012). Integrated salinity reduction and water recovery in an osmotic microbial desalination cell. *RSC Adv.* 2:3265. doi: 10.1039/c2ra20193c
- Zhang, B., Zheng, X., Voznyy, O., Comin, R., Bajdich, M., García-Melchor, M., et al. (2016). Homogeneously dispersed multimetal oxygen-evolving catalysts. *Science* 352, 333–337. doi: 10.1126/science.aaf1525
- Zhang, F., Chen, M., Zhang, Y., and Zeng, R. J. (2012). Microbial desalination cells with ion exchange resin packed to enhance desalination at low salt concentration. *J. Memb. Sci.* 417–418, 28–33. doi: 10.1016/j.memsci.2012.06.009
- Zhang, F., and He, Z. (2015). Scaling up microbial desalination cell system with a post-aerobic process for simultaneous wastewater treatment and seawater desalination. *Desalination* 360, 28–34. doi: 10.1016/j.desal.2015.01.009

- Zhao, F., Harnisch, F., Schröder, U., Scholz, F., Bogdanoff, P., and Herrmann, I. (2006). Challenges and constraints of using oxygen cathodes in microbial fuel cells. *Environ. Sci. Technol.* 40, 5193–5199. doi: 10.1021/es060332p
- Zuo, K., Chang, J., Liu, F., Zhang, X., Liang, P., and Huang, X. (2017). Enhanced organics removal and partial desalination of high strength industrial wastewater with a multi-stage microbial desalination cell. *Desalination* 423, 104–110. doi: 10.1016/j.desal.2017.09.018
- Zuo, K., Chen, M., Liu, F., Xiao, K., Zuo, J., Cao, X., et al. (2018). Coupling microfiltration membrane with biocathode microbial desalination cell enhances advanced purification and long-term stability for treatment of domestic wastewater. *J. Memb. Sci.* 547, 34–42. doi: 10.1016/j.memsci.2017.10.034

Conflict of Interest: The authors declare that the research was conducted in the absence of any commercial or financial relationships that could be construed as a potential conflict of interest.

Copyright © 2019 Ramírez-Moreno, Rodenas, Aliaguilla, Bosch-Jimenez, Borràs, Zamora, Monsalvo, Rogalla, Ortiz and Esteve-Núñez. This is an open-access article distributed under the terms of the Creative Commons Attribution License (CC BY). The use, distribution or reproduction in other forums is permitted, provided the original author(s) and the copyright owner(s) are credited and that the original publication in this journal is cited, in accordance with accepted academic practice. No use, distribution or reproduction is permitted which does not comply with these terms.